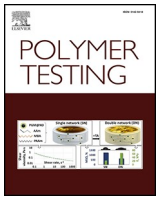
Polymer Testing 153 (2025) 109049



Contents lists available at ScienceDirect

Polymer Testing

journal homepage: www.elsevier.com/locate/polytest



Design of high-performance phase change composites using erythritol-modified epoxy/docosane and cellulose-grafted spherical aluminum nitride

Wondu Lee [a,1], Min Park [d,1], Pei-Chen Su [c], Jooheon Kim [a,b,*]

[a] Department of Chemical Engineering, Chung-Ang University, Seoul, 156-756, Republic of Korea
[b] Graduate School of Intelligence Energy and Industry, Chung-Ang University, Seoul, 06974, Republic of Korea
[c] School of Mechanical and Aerospace Engineering, Nanyang Technological University, 50 Nanyang Avenue, Singapore, 639798, Singapore
[d] Manufacturing Core Technology Team, Global Technology Research, Samsung Electronics, Republic of Korea

ARTICLE INFO

Keywords:
Polymer-matrix composites (PMCs)
Phase change materials (PCMs)
Latent heat
Thermal conductivity

ABSTRACT

The increasing demand for efficient thermal regulation in high-power electronic devices necessitates the development of advanced thermal interface materials. In this work, a novel composite was fabricated to address this challenge. The foundational material, an epoxy–erythritol (EPET) matrix, was synthesized by chemically grafting a phase-change material (PCM) onto an epoxy base, resulting in a single endothermic transition within the range of 110–124 °C. To broaden the thermal response, docosane was introduced, producing an EPET/docosane hybrid system that exhibited multiple endothermic transitions in the ranges of 40–60 °C and 110–124 °C. To enhance heat transfer performance, spherical aluminum nitride (AlN) was incorporated as a thermally conductive filler. The AlN particles were surface-modified with cellulose nanofiber (CNF) to improve interfacial adhesion with the polymer matrix and promote efficient thermal transport. The optimized composite, EPET/Docosane/AlN-CNF, achieved a thermal conductivity of 6.31 W/m·K and a total latent heat of 130.7 J/g. When applied to a CPU, the composite demonstrated superior heat-buffering capability, attributed to its dual endothermic transitions and high latent heat. These findings validate the potential of the developed composite as a high-performance thermal interface material for next-generation electronic devices.

1. Introduction

Electronic technologies have become indispensable in both everyday applications and advanced industries, encompassing systems from portable devices such as smartphones [1] and laptops [2] to highly specialized platforms in aerospace [3] and electric vehicle engineering [4]. The relentless drive toward miniaturization, improved efficiency, and enhanced computational power has significantly increased heat generation, making thermal management a critical determinant of system performance and durability [5,6]. Inadequate heat dissipation not only accelerates material degradation and shortens service life but also hinders the advancement of next-generation high-power electronics. Consequently, effective thermal control has become central to sustaining technological progress [7,8].

As electronic devices continue to shrink while delivering greater computational output, conventional cooling strategies, such as metallic heat sinks and forced-air convection, are approaching their performance limits [9,10]. These traditional methods, which rely primarily on conductive and convective heat transfer, were sufficient for earlier hardware generations but are increasingly inadequate in addressing the elevated power densities and spatial constraints of modern miniaturized systems. This disparity between heat generation and dissipation underscores the urgent need for innovative thermal management solutions [11–13].

Thermal interface materials (TIMs) have become essential for temperature control in electronic devices, with polymer-based composites emerging as one of the most extensively studied classes [14,15]. Common polymer matrices, such as epoxy resins [16], polyvinyl alcohol [17], and cellulose nanofibers derived from biological sources [18], offer advantages including low weight, facile processability, and cost

* Corresponding author. Department of Chemical Engineering, Chung-Ang University, Seoul, 156-756, Republic of Korea
E-mail address: jooheonkim@cau.ac.kr (J. Kim).
[1] Equally contributed to this paper.

https://doi.org/10.1016/j.polymertesting.2025.109049
Received 27 August 2025; Received in revised form 6 November 2025; Accepted 14 November 2025
Available online 15 November 2025
0142-9418/© 2025 The Authors. Published by Elsevier Ltd. This is an open access article under the CC BY-NC-ND license (http://creativecommons.org/licenses/by-nc-nd/4.0/).

efficiency. However, their intrinsic thermal conductivity, typically below 0.5 W/m·K, limits their effectiveness in heat dissipation when used alone [19]. To overcome this limitation, these polymers are often reinforced with thermally conductive fillers such as boron nitride (BN) [20], aluminum nitride (AlN) [21], and graphene [22]. While such fillers enhance thermal transport, ceramic-based TIMs still face significant challenges: at practical filler loadings, the overall thermal conductivity remains moderate, and excessive addition can compromise both processability and structural integrity, critical concerns for applications requiring simultaneous electrical insulation and efficient heat spreading.

In this context, phase-change materials (PCMs) have attracted considerable interest as functional additives in advanced TIMs. Organic PCMs, including paraffin [23], stearic acid [24], and palmitic acid (PA) [25], dynamically regulate temperature by absorbing and releasing latent heat during reversible solid–liquid transitions. When incorporated into composite matrices, PCMs enable the development of phase-change TIMs (PCTIMs) that integrate structural flexibility with thermal buffering capabilities. These systems represent a promising strategy to surpass the intrinsic thermal conductivity limitations of polymer/ceramic composites, offering high-performance, reversible thermal management tailored for compact, high-power electronic devices.

In contrast to conventional heat-dissipation materials that primarily operate through conductive heat transfer, organic PCMs leverage the latent heat associated with thermally induced phase transitions. These materials undergo reversible solid–liquid transformations within a defined temperature range, during which significant amounts of thermal energy are absorbed or released. This phase-transition behavior endows organic PCMs with exceptional thermal energy storage capacity, making them effective for moderating temperature fluctuations in thermal management applications.

Ongoing research increasingly focuses on the development and integration of PCTIMs across a broad spectrum of electronic systems. These efforts encompass the synthesis and molecular tailoring of organic PCMs, their physicochemical characterization, and strategies for embedding them into composite structures compatible with practical electronic architectures. However, several technical challenges hinder the widespread implementation of PCTIMs in advanced electronics. Key concerns include ensuring material compatibility, preserving structural integrity under extended operational stress, and achieving long-term reliability under cyclic thermal and mechanical loading. Addressing these challenges is critical to the successful deployment of organic PCMs in high-performance and environmentally demanding electronic applications [26,27].

A fundamental drawback of PCMs is their tendency to leak during the solid–liquid transition, which restricts their practical applications. A common strategy to mitigate this issue involves physically embedding encapsulated PCM particles within polymer matrices. Although the encapsulating shell effectively prevents leakage, the physical dispersion of individual capsules introduces numerous interfaces between the PCM and the matrix. These interfacial boundaries reduce the overall latent heat capacity of the composite and adversely affect its thermal and mechanical performance.

In this study, erythritol (ET) was chemically grafted onto EP to form an EPET matrix, into which docosane was subsequently incorporated. To establish a heat transfer pathway along the through-plane direction and enhance thermal conductivity, CNF-grafted AlN was introduced, and the resulting EPET/docosane/AlN-CNF composite was fabricated via a hot-pressing method. The hydrophilic hydroxyl groups of CNF on the AlN surface facilitated hydrogen bonding between the fillers and the matrix, thereby improving interfacial interactions. The synthesized EPET/docosane/AlN-CNF composite exhibits exceptional thermal properties, making it a promising PCTIM. It displays dual endothermic transitions and a high latent heat, confirming its effectiveness in thermal energy absorption and storage. In leakage tests, the material demonstrated excellent thermal stability, maintaining structural integrity up to 180 °C without signs of degradation, a critical factor for long-term reliability in electronic devices. When applied to a CPU, the composite's thermal management performance was further validated. These results confirm that the material offers superior functionality as a PCTIM, presenting an effective solution to the thermal challenges in modern electronics.

2. Results and discussion

2.1. Fabrication and characterization of the PCM

The synthesis of the EPET/docosane/AlN-CNF composite is outlined in Fig. 1. The process was specifically designed to address key challenges associated with fabricating PCMs, particularly their low mechanical strength and tendency to leak. A two-step approach was employed: first, ET was chemically grafted onto the epoxy resin (EP) backbone. This step was essential due to the inherently low compatibility between EP and ET, which often leads to phase separation. Through an esterification reaction, a stable, chemically bonded EPET polymer network was successfully formed. Subsequently, docosane was incorporated into the matrix to complete the composite fabrication. This structural design enhances mechanical integrity and effectively prevents PCM leakage, a common limitation in conventional systems.

The successful synthesis of the EPET composite was confirmed using Fourier-transform infrared (FT-IR) spectroscopy (see Fig. 2). D-230 of amine-based curing agent was chosen for grafting the ET via ring-opening reactions of epoxy groups, which formed ester bonds and grafted highly reactive hydroxyl groups onto the polymer backbone. The curing agents can initiate epoxy ring-opening reactions by nucleophilic addition leading to the formation of a strong three-dimensional cross-linked network. Curing agents of epoxies can be di/polyamines (aliphatic or cycloaromatic), anhydrides, alcohols, phenols, and carboxylic acids. As the curing reaction progressed, the concentrations of anhydride groups decreased, causing some hydroxyl groups of ET to participate in the ring opening of the epoxy groups [28–30]. The spectrum exhibited characteristic shifts in the key peaks of EP and ET, along with the emergence of a new absorption band at 1608 cm^{-1}, indicative of ester bond formation. Additionally, the disappearance of the peak at 913 cm^{-1} confirmed the ring-opening of the epoxy groups, verifying that ET chains were successfully and permanently grafted onto the EP network.

Differential scanning calorimetry (DSC) was subsequently employed to evaluate the thermal properties of the composite. While pure ET exhibits a sharp melting point at 126 °C, the EPET composite displayed a broader melting range from 110 °C to 124 °C, with a peak at 119.5 °C. This decrease in melting point is attributed to the grafting process, which reduced the number of free hydroxyl groups responsible for extensive hydrogen bonding, thereby lowering the thermal transition temperature. These thermal changes further substantiate the successful incorporation of ET into the EP network.

The mechanical and thermal properties of the composite were evaluated, as summarized in Table 1. The EPET matrix exhibited a substantial improvement in mechanical performance, with tensile strength increasing by over 350 % and strain exceeding 40 %, significantly surpassing that of pure ET. Despite these mechanical enhancements, the composite with a 2:1 ET:EP ratio retained 70 % of its latent heat capacity without notable degradation. These results confirm that the EPET matrix functions as a promising PCM, offering a balanced combination of mechanical robustness and thermal performance.

The cross-sectional morphology of the cured EPET composite was examined using Field-Emission Scanning Electron Microscopy (FE-SEM), as shown in Fig. 3a–d. The EPET sample exhibited a uniform and homogeneous cross-section, indicating successful component integration without phase separation. This contrasts sharply with a physically mixed sample of EP and ET, which displayed distinct phase boundaries and incomplete blending, confirming poor compatibility. Furthermore, upon incorporation of docosane into the EPET matrix, the material

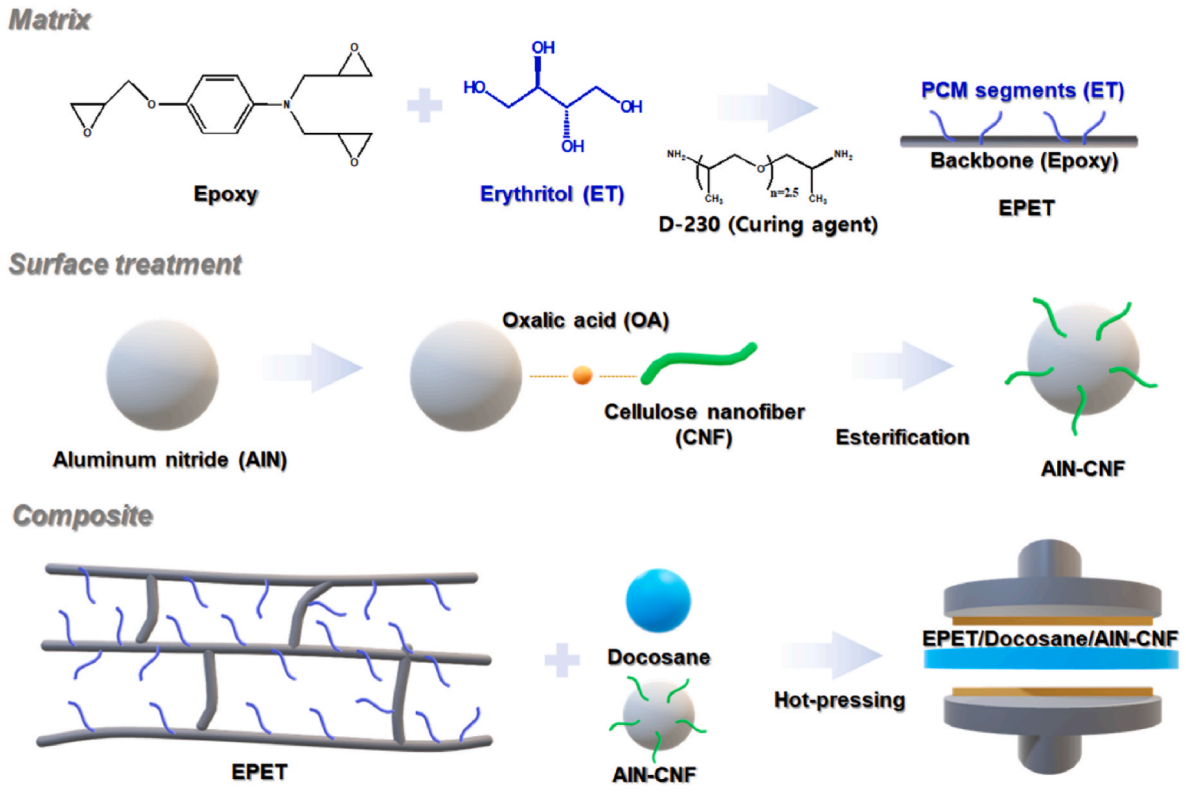


Fig. 1. Schematic illustration of the EPET/docosane/AlN composite structure.

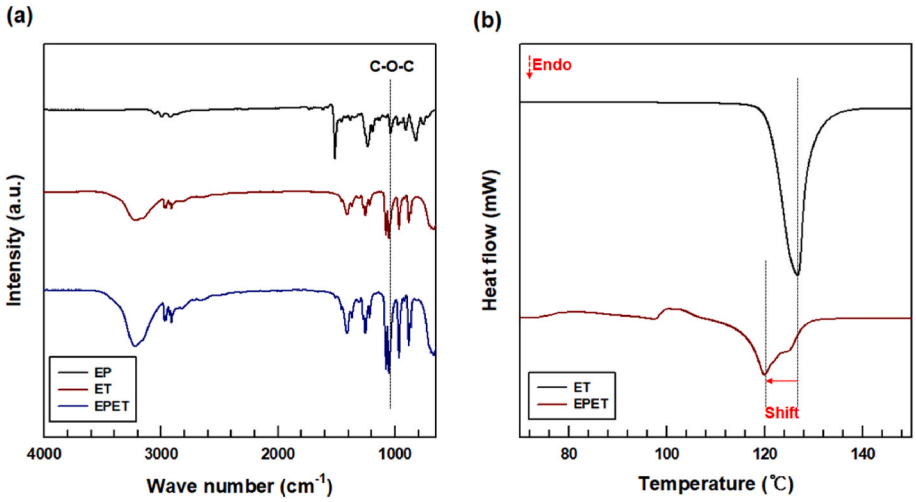


Fig. 2. (a) FT-IR spectra and (b) DSC curves of the matrices during ET grafting.

Table 1
Properties of EPET at various ratios.

Ratio (EP: ET)	Tensile strength (MPa)	Elongation at break (%)	Latent heat (J/g)
0:1 (pure ET)	0.65	1.16	390
2:1	4.76	3.5	82.53
1:1	3.22	2.77	179.16
1:1.5	2.56	1.94	230.42
1:2	2.03	1.55	275.97

maintained a highly homogeneous structure, with docosane well-dispersed throughout. These morphological observations provide compelling visual evidence of effective chemical bonding and uniform dispersion within the composite.

2.2. Characterization of AlN-CNF

FT-IR analysis was conducted to investigate chemical bond modifications resulting from the surface treatment process. Following the reaction between AlN and CNFs, the FT-IR spectrum of the AlN–CNF composite displayed new absorption bands, most notably the O–H stretching vibration at 3280 cm^{-1}. Additionally, the carbonyl (C=O) stretching vibration of ester groups, originally observed at 1715 cm^{-1},

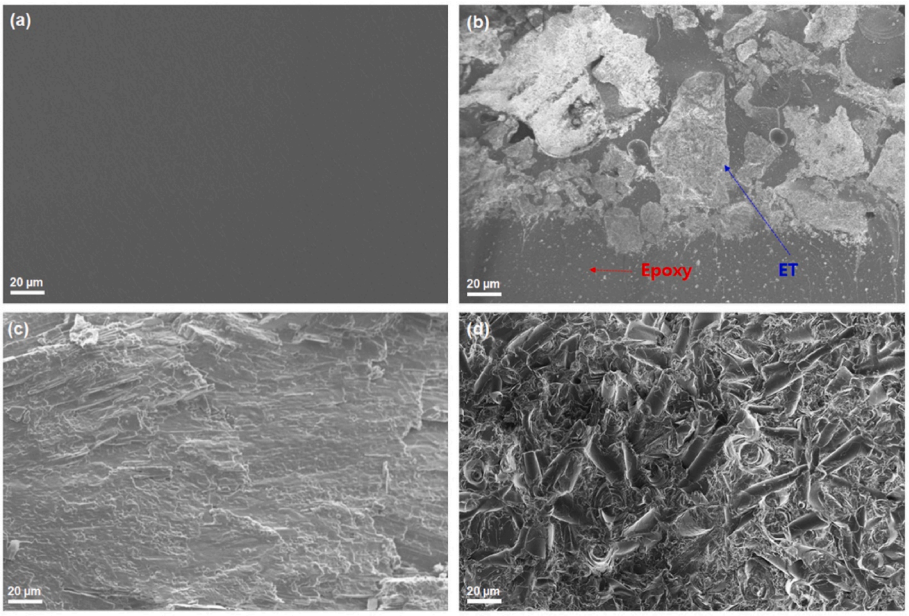


Fig. 3. Morphologies of (a) EP, (b) physically mixed EP/ET, (c) EPET, and (d) EPET/Docosane.

shifted to 1731 cm^{-1}. These spectral changes confirm successful esterification, indicating effective grafting of CNFs onto the AlN surface.

TGA (Fig. 4(b)) was employed to quantify the grafting ratio of oxygen-containing functional groups and CNFs on the AlN surface. A minor weight loss of approximately 0.5 % below 220 °C was attributed to moisture evaporation from the CNFs, while thermal degradation of CNFs began above 220 °C. Notably, the AlN–CNF sample exhibited a 9 % weight reduction at 800 °C compared to pure AlN, further supporting the successful grafting of CNFs and oxygen-containing functional groups.

FE-SEM images (Fig. 4(c–e)) were analyzed to examine morphological changes in the fillers. The pristine spherical structure of AlN was retained after grafting (Fig. 4(c and d)), and a higher magnification image (Fig. 4(e)) clearly shows CNFs adhered to the AlN surface, providing visual confirmation of successful grafting without compromising the original morphology.

2.3. Morphology of composites

The internal structure of the high-performance PCM composites,

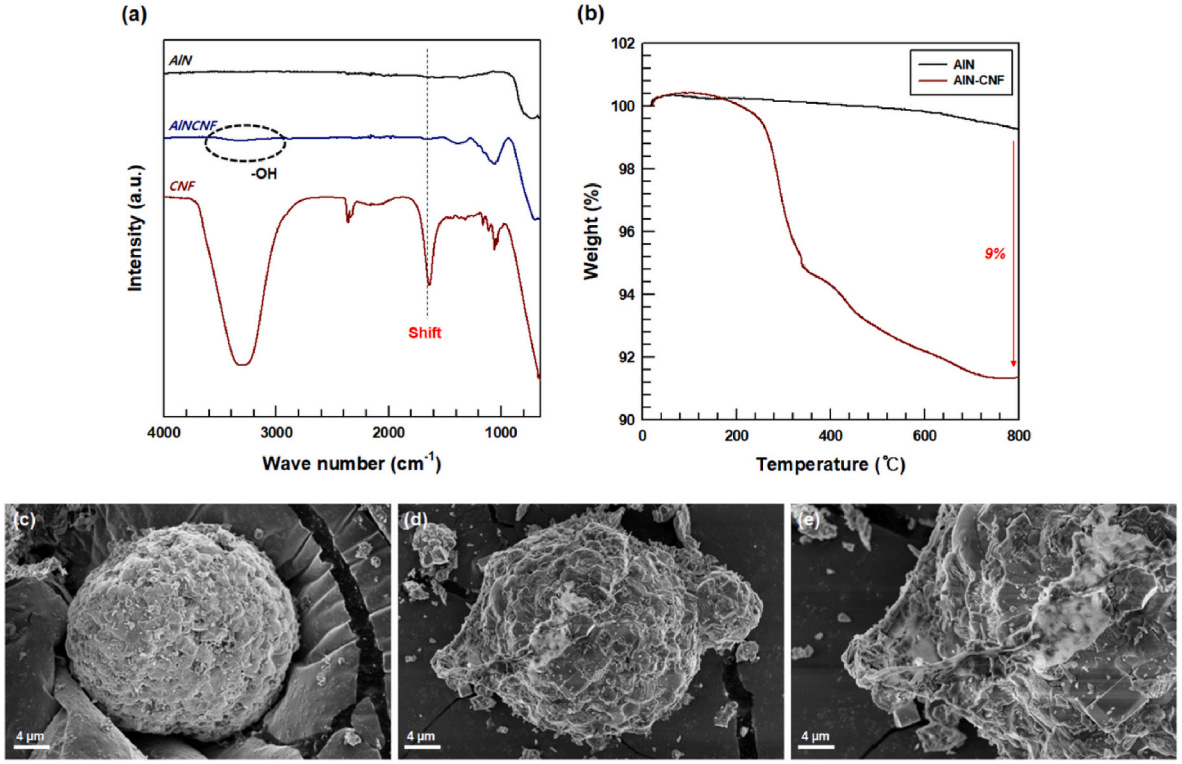


Fig. 4. (a) FT-IR spectra, (b) TGA curves, and (c–e) morphologies as a function of CNF treatment on the AlN surface.

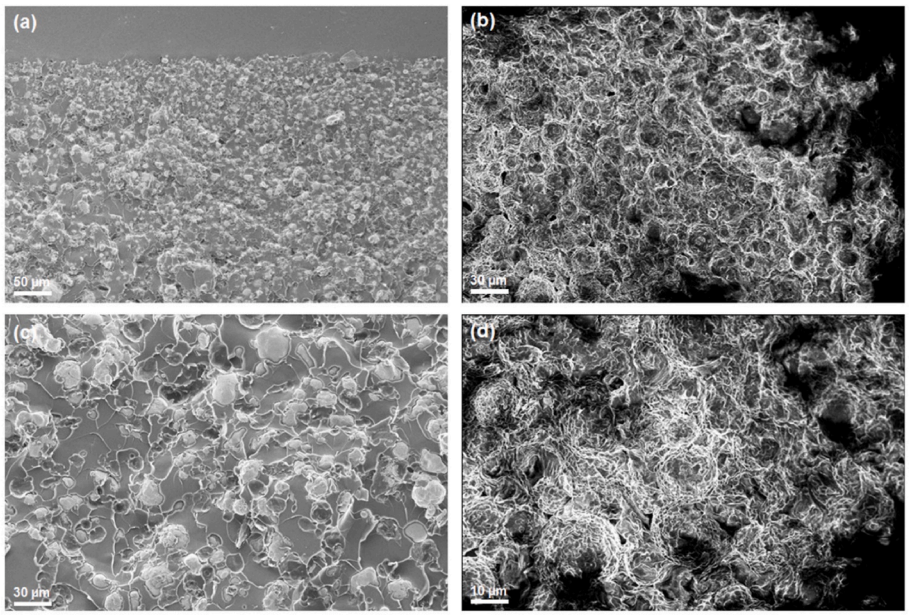


Fig. 5. Morphologies of (a, c) EPET/Docosane/AlN (Filler loading: 60 wt %) and (b, d) EPET/Docosane/AlN-CNF (Filler loading: 60 wt %).

fabricated by incorporating AlN–CNF into the EPET/Docosane matrix, was analyzed using FE-SEM (Fig. 5). A critical distinction was observed between composites containing raw AlN and those with CNF-treated AlN. As shown in Fig. 5(a) and (c), the composites with raw AlN exhibited significant particle aggregation and a distinct interface between the AlN and the matrix, indicating poor interfacial adhesion. In

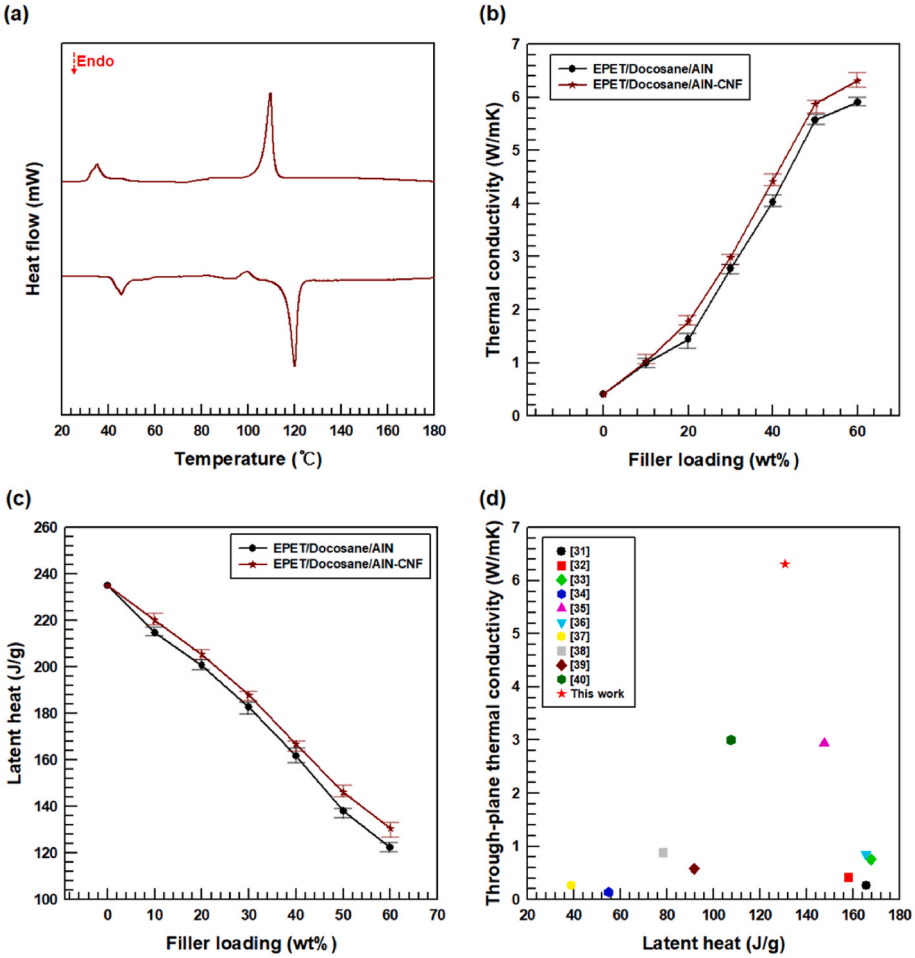


Fig. 6. (a) DSC curve of EPET composite. (b) Thermal conductivity, (c) latent heat of the composites, and (d) comparison with previously reported values [31–40].

contrast, Fig. 5(b) and (d) demonstrate that CNF treatment on the AlN surface markedly improved adhesion between the filler and the matrix. This enhancement is attributed to hydrogen bonding between the CNF-coated AlN and the polymer matrix, promoting more uniform dispersion and forming a stronger structural network.

2.4. Properties

The thermal behavior of the EPET/Docosane/AlN–CNF composite was thoroughly analyzed using DSC. At around 40–50 °C in Fig. 6(a), docosane begins to change phase and begins to absorb heat first, and from 110 °C, the crystallized ET grafted onto the epoxy backbone begins to absorb heat secondarily and liquefy. This dual PCM system enables the material to absorb heat and regulate temperature across two distinct temperature ranges, providing enhanced thermal buffering for electronic devices operating under variable thermal loads. To evaluate thermal performance, key properties such as specific heat capacity, density, and through-plane thermal diffusivity were measured. In other words, Efficient heat transfer paths were formed by improvement in interfacial adhesion between AlN-CNF fillers and EPET matrix due to inducing hydrogen bonding between the hydroxyl groups of AlN surface and the hydroxyl groups of EPET. Based on this, The EPET/Docosane/AlN–CNF composite achieved a thermal conductivity of 6.31 W/m·K, representing a 1260 % enhancement over pure ET (Fig. 6(b) and Fig. S2 (a))). This substantial improvement results from a deliberate design strategy. CNF treatment on the AlN particles facilitated the formation of highly efficient, interconnected heat-transfer pathways aligned in the through-plane direction. Combined with the high density achieved through hot pressing, this alignment produced a synergistic effect that significantly enhanced the composite's ability to dissipate heat.

The latent heat of a PCM is a critical parameter for evaluating its capacity to store and release thermal energy. As shown in Fig. 6(c) and Fig. S2(b), the latent heat of the EPET/Docosane/AlN–CNF composite was measured at various filler concentrations. The results were highly favorable, with the composite achieving a peak latent heat of 130.7 J/g at a 60 wt % AlN–CNF loading. This high latent heat capacity indicates the material can absorb substantial thermal energy with minimal temperature rise, making it well-suited for mitigating thermal fluctuations.

A comprehensive comparison with recently reported PCM-based thermal management materials is presented in Fig. 6(d) [31–40]. This analysis highlights the superior performance of the composite in terms of both thermal conductivity and latent heat. The synergistic combination of high latent heat, excellent thermal conductivity, and dual-stage endothermic transitions positions the EPET/Docosane/AlN–CNF composite as a promising candidate for next-generation electronic thermal management systems. In addition to demonstrating the effectiveness of the fabrication approach, this work establishes a new benchmark for high-performance thermal interface materials.

A leakage test was conducted to evaluate the structural stability of the EPET/Docosane/AlN–CNF composite under elevated temperatures (Fig. 7(a)). To quantitatively assess leakage, the retention rate (ε) and leakage rate (γ) were calculated using the following equations:

$$\varepsilon = m_r/m_0 \times 100\ \%, \quad (1)$$

$$\gamma = (m_0 - m_r)/m_0 \times 100\ \%, \quad (2)$$

Where ε represents the PCM retention rate, γ is the leakage rate, m_0 is the initial mass of the sample, and m_r is the mass measured at a specific time. These metrics are critical for evaluating the composite's containment performance and thermal stability.

Experimental results revealed a marked contrast between the composite and pure ET. When heated above its melting point of 125 °C, pure ET exhibited a sharp decline in retention rate. At 160 °C, the ET sample fully melted and leaked, resulting in a 0 % retention rate and complete structural failure.

In stark contrast, the EPET/Docosane composite exhibited significantly greater thermal stability, showing only a slight reduction in retention beginning around 150 °C. The EPET/Docosane/AlN–CNF composite demonstrated even more robust performance, with virtually no leakage observed up to 180 °C; at this elevated temperature, the retention rate remained as high as 98.5 %. This exceptional stability provides direct evidence that chemical grafting of ET onto the epoxy matrix effectively reinforces the composite structure, preventing PCM leakage even at temperatures well above the melting point. The successful integration of the AlN–CNF filler further enhances this thermal resilience.

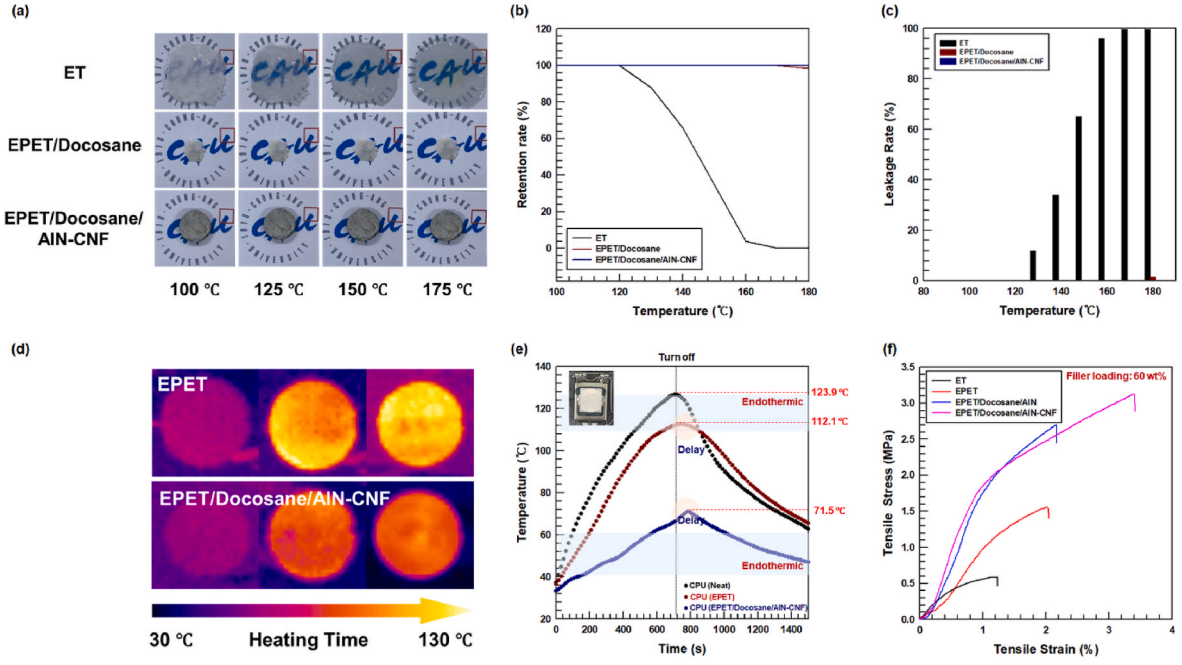


Fig. 7. (a) Leakage test, (b) retention rate, and (c) leakage rate of ET, EPET/Docosane, and EPET/Docosane/AlN-CNF, as determined through leakage testing. (d) Results of thermal management tests on a CPU module. (e) Mechanical properties of the composites.

To evaluate the composite's thermal regulation performance, infrared thermographic imaging was employed. Fig. 7(d) and (e) illustrate the heat management behavior of the EPET/Docosane/AlN–CNF composite when applied to a CPU under localized thermal loading. Surface temperature was monitored over a 600 s period to assess the composite's effectiveness in dissipating heat.

The thermal regulation performance was compared directly among a bare CPU, a CPU coated with only the EPET matrix, and one using the full EPET/Docosane/AlN–CNF composite. As expected, the bare CPU exhibited a rapid and uncontrolled temperature rise. In contrast, both the EPET matrix and the full composite substantially delayed this increase.

The superior performance of the composite is attributed to its dual-stage thermal buffering effect, which arises from the latent heat absorption of two distinct PCMs: the grafted PCM chains and the incorporated docosane. This mechanism enables the composite to temporarily sequester thermal energy from the CPU, thereby effectively delaying heat accumulation.

Among the tested materials, the EPET/Docosane/AlN-CNF composite demonstrated the highest effectiveness. The synergistic combination of grafted PCM chains and docosane yields a performance advantage over conventional PCM-loaded systems, validating its potential as a leading thermal interface material for future high-power electronic devices.

Mechanical characterization using UTM (Fig. 7(e)) showed that the incorporation of fillers significantly enhanced the composite's tensile strength and elongation, increasing from 2.03 MPa to 3.39 MPa and from 1.55 % to 3.13 %, respectively. These improvements are attributed to the brittle nature of AlN, which facilitates stress transfer. Furthermore, CNF-functionalized AlN exhibited superior mechanical performance, consistent with trends observed in thermal conductivity, suggesting that mechanical strengthening also results from a robust AlN–CNF network effectively embedded within the polymer matrix.

3. Conclusions

In this study, we successfully developed a novel phase-change thermal interface material (PCTIM) for efficient thermal management in electronic devices. The composite, EPET/Docosane/AlN-CNF, is distinguished by its dual endothermic behavior, which effectively decelerates device temperature rise. This was achieved by incorporating two types of PCMs, one chemically grafted and the other physically dispersed, into an epoxy matrix, resulting in endothermic transitions within the ranges of 40–60 °C and 110–124 °C. In addition to its thermal buffering capability, the composite exhibited significantly enhanced thermal conductivity. Surface modification of AlN with CNF improved interfacial adhesion with the epoxy matrix via hydrogen bonding, enabling uniform dispersion of AlN-CNF particles and the formation of efficient heat conduction pathways in the through-plane direction. The resulting EPET/Docosane/AlN-CNF composite demonstrates a strong synergy between latent heat absorption and enhanced heat dissipation, confirming its substantial potential as a high-performance PCTIM for advanced thermal management applications.

CRediT authorship contribution statement

Wondu Lee: Writing – original draft, Validation, Methodology, Investigation, Formal analysis, Data curation, Conceptualization. **Min Park:** Writing – original draft, Validation, Methodology, Investigation, Formal analysis, Data curation, Conceptualization. **Pei-Chen Su:** Formal analysis, Data curation. **Jooheon Kim:** Supervision, Project administration, Funding acquisition.

Declaration of competing interest

The authors declare that they have no known competing financial interests or personal relationships that could have appeared to influence the work reported in this paper.

Acknowledgement

This work was supported by Korea Institute of Energy Technology Evaluation and Planning (KETEP) grant funded by the Korea government (MOTIE) RS-2024-00398346, ESS BigData-Based O&M and Asset Management Technical Manpower Training) and the National Research Foundation of Korea (NRF) grant funded by the Korea government (MSIT) (NRF-2022M3H4A1A02076956).

Appendix A. Supplementary data

Supplementary data to this article can be found online at https://doi.org/10.1016/j.polymertesting.2025.109049.

Data availability

Data will be made available on request.

References

[1] S. Yuan, L. Long, K. Xu, P. Zuo, Z. Ye, X. Meng, J. Zhu, H. Ye, Multi-objective optimization of thermal modules in high heat flux laptops, Appl. Therm. Eng. 239 (2024).
[2] T. Hu, J. Zhang, W. Chan, R. Xiao, H. Xu, X. Zhao, G. Wang, W. Yu, Synthesis and optimization of GO/TiO2@n-octadecane microcapsules for thermal management of smartphone charging, Appl. Therm. Eng. 257 (2024).
[3] T. Chen, T. Tokuyama, Y. Ko, T. Hiroyuki, K. Matsubara, Y. Nakahara, K. Narita, A. Nishihara, A. Namba, T. Muraki, K. Asai, T. Araki, S. Tanaka, Double-side direct oil-cooling automotive power module: from material compatibility to thermal management, IEEE Trans. Ind. Appl. (2025) 1–12.
[4] O. Aghababaei Tafreshi, Z. Saadatnia, S. Ghaffari-Mosanenzadeh, M. M. Rastegardoost, C. Zhang, C.B. Park, H.E. Naguib, Polyimide aerogel fiber bundles for extreme thermal management systems in aerospace applications, ACS Appl. Mater. Interfaces 16 (40) (2024) 54597–54609.
[5] C. Wu, Y. Sun, H. Tang, S. Zhang, W. Yuan, L. Zhu, Y. Tang, A review on the liquid cooling thermal management system of lithium-ion batteries, Appl. Energy 375 (2024).
[6] X. Zhang, K. Sun, H. Liu, J. Chen, X. Yan, Y. Kou, Q. Shi, Flexible insulating phase change composite film with improved thermal conductivity for wearable thermal management, Nano Energy 121 (2024).
[7] G. Leoncini, R. Mothier, B. Michel, M. Clausse, A review on challenges concerning thermal management system design for medium duty electric vehicles, Appl. Therm. Eng. 236 (2024).
[8] J. Deng, Q. Huang, X. Li, G. Zhang, C. Li, S. Li, Influence mechanism of battery thermal management with flexible flame retardant composite phase change materials by temperature aging, Renew. Energy 222 (2024).
[9] H. Niu, H. Guo, L. Kang, L. Ren, R. Lv, L. Liu, A. Bashir, S. Bai, Highly thermally conductive and soft thermal interface materials based on vertically oriented boron nitride film, Compos. B Eng. 272 (2024).
[10] J. Lee, W. Park, Investigation of thermal transport across volume-controlled thermal interface materials, Polym. Test. 146 (2025).
[11] Z. Lin, H. Jin, H. Deng, Z. Zu, H. Huang, L. Zhang, H. Xiang, Robust, self-healable, recyclable and thermally conductive silicone composite as intelligent thermal interface material, Compos. Struct. 332 (2024).
[12] X. Kong, Y. Chen, R. Yang, Y. Wang, Z. Zhang, M. Li, H. Chen, L. Li, P. Gong, J. Zhang, K. Xu, Y. Cao, T. Cai, Q. Yan, W. Dai, X. Wu, C.-T. Lin, K. Nishimura, Z. Pan, N. Jiang, J. Yu, Large-scale production of boron nitride nanosheets for flexible thermal interface materials with highly thermally conductive and low dielectric constant, Compos. B Eng. 271 (2024).
[13] G. Liu, K. Shang, S. Chen, J. Shen, Macro/Micro synergistic thermal conductivity enhancement in liquid metal-based phase change composites for thermal management in electronic devices, Compos. Sci. Technol. 264 (2025).
[14] C. Wang, Q. Lin, Z. Pan, J. Hong, Y. Zhou, Thermal contact analysis of flip-chip package considering microscopic contacts of double-layer thermal interface materials, Appl. Energy 356 (2024).
[15] S. Chakraborty, D. Shukla, P. Kumar Panigrahi, A review on coolant selection for thermal management of electronics and implementation of multiple-criteria decision-making approach, Appl. Therm. Eng. 245 (2024).
[16] Z. Liu, M. Wang, T. Wang, Y. Tian, J. Cheng, J. Zhang, Epoxy resin-based gel phase change material for strong interface bonding and interface thermal management, Chem. Mater. 36 (19) (2024) 9414–9423.
[17] X. Yang, Y. Wang, H. Cong, Y. Fang, S. Chen, C. Yan, H. Deng, Construction of tree-ring mimetic 3D networks in polyvinyl alcohol/boron nitride composites for enhanced thermal management and mechanical properties, Polymer 311 (2024).

[18] C. Zeng, H. Wang, F. Bu, Q. Cui, J. Li, Z. Liang, L. Zhao, C. Yi, A regenerated cellulose fiber with high mechanical properties for temperature-adaptive thermal management, Int. J. Biol. Macromol. 274 (Pt 2) (2024) 133550.
[19] S. Jiong, J. Yun, J. Lee, J. Kim, Y. Choi, T. Kim, D. Lee, H. Eom, W. Choi, Nanosized boron nitride-incorporated polyvinyl alcohol composites with TEMPO-Oxidized cellulose nanofibers as ultrathin thermal interface materials, Chem. Eng. J. 500 (2024).
[20] R. Yang, Y. Wang, Z. Zhang, K. Xu, L. Li, Y. Cao, M. Li, J. Zhang, Y. Qin, B. Zhu, Y. Guo, Y. Zhou, T. Cai, C.T. Lin, K. Nishimura, C. Xue, N. Jiang, J. Yu, Highly oriented BN-based TIMs with high through-plane thermal conductivity and low compression modulus, Mater. Horiz. 11 (17) (2024) 4064–4074.
[21] Y. Liu, Q. Lin, X. Long, S. Zhang, H. Dong, Y. Song, C. Wu, Effect of segment structure of monotrimethoxysilylethyl-terminated asymmetric polysiloxanes on the thermal management performance of AlN-filled silicone pastes, React. Funct. Polym. 198 (2024).
[22] K. Huang, S. Pei, Q. Wei, Q. Zhang, J. Guo, C. Ma, H.M. Cheng, W. Ren, Highly thermally conductive and flexible thermal interface materials with aligned graphene lamella frameworks, ACS Nano 18 (34) (2024) 23468–23476.
[23] M.G. Kibria, M.S. Mohtasim, U.K. Paul, B.K. Das, R. Saidur, Impact of hybrid nano PCM (paraffin wax with Al2O3 and ZnO nanoparticles) on photovoltaic thermal system: energy, exergy, exergoeconomic and enviroeconomic analysis, J. Clean. Prod. 436 (2024).
[24] Q. Tan, H. Liu, Y. Shi, M. Zhang, B. Yu, Y. Zhang, Lauric acid/stearic acid/nano-particles composite phase change materials for energy storage in buildings, J. Energy Storage 76 (2024).
[25] W. Lee, J. Kim, Poly(dimethylsiloxane) grafting on palmitic acid and surface of expanded graphite for advanced phase change material composites, J. Storage Mater. 52 (2022).
[26] W. Lee, J. Kim, A comprehensive review of research on organic-based phase-change thermal interface materials for thermal management of electric devices: methods, performance, and applications, Polym. Test. 142 (2025) 108577.
[27] W. Lee, J. Hong, J. Song, W. Yang, J. Kim, Fabrication of high-performance thermally conductive phase change material composites with porous ceramic filler network for efficient thermal management, Compos. Sci. Technol. 240 (2023) 110092.
[28] C.P. Pappa, S. Torofias, K.S. Triantafyllidis, Sub-micro organosolv lignin as bio-based epoxy polymer component: a sustainable curing agent and additive, ChemSusChem 16 (13) (2023) e202300076.
[29] X. Zhen, X. Cui, A. Al-Haimi, X. Wang, H. Liang, Z. Xu, Z. Wang, Fully bio-based epoxy resins from lignin and epoxidized soybean oil: rigid-Flexible, tunable properties and high lignin content, Int. J. Biol. Macromol. 254 (Pt 2) (2024) 127760.
[30] Z. Huang, Q. Ye, Z. Shi, J.-N. Tang, X. Ouyang, D.-Z. Chen, Multiple phase change-stimulated shape memory and self-healing epoxy composites with thermal regulation function, Chem. Eng. J. 409 (2021).
[31] M. George, A.K. Pandey, N. Abd Rahim, V.V. Tyagi, S. Shahabuddin, R. Saidur, A novel polyaniline (PANI)/paraffin wax nano composite phase change material: superior transition heat storage capacity, thermal conductivity and thermal reliability, Sol. Energy 204 (2020) 448–458.
[32] X. Sheng, D. Dong, X. Lu, L. Zhang, Y. Chen, MXene-wrapped bio-based pomelo peel foam/polyethylene glycol composite phase change material with enhanced light-to-thermal conversion efficiency, thermal energy storage capability and thermal conductivity, Compos. A. Appl Sci. Manuf. 138 (2020).
[33] N. Tan, T. Xie, Y. Feng, P. Hu, Q. Li, L.-M. Jiang, W.-B. Zeng, J.-L. Zeng, Preparation and characterization of erythritol/sepiolite/exfoliated graphite nanoplatelets form-stable phase change material with high thermal conductivity and suppressed supercooling, Sol. Energy Mater. Sol. Cells 217 (2020).
[34] A. Bashiri Rezaie, M. Montazer, Shape-stable thermo-responsive nano Fe3O4/fatty acids/PET composite phase-change material for thermal energy management and saving applications, Appl. Energy 262 (2020).
[35] D. Liu, C. Lei, K. Wu, Q. Fu, A multidirectionally thermoconductive phase change material enables high and durable electricity via real-environment solar-thermal-electric conversion, ACS Nano 14 (11) (2020) 15738–15747.
[36] C. Shen, X. Li, G. Yang, Y. Wang, L. Zhao, Z. Mao, B. Wang, X. Feng, X. Sui, Shape-stabilized hydrated salt/paraffin composite phase change materials for advanced thermal energy storage and management, Chem. Eng. J. 385 (2020).
[37] Z. Qian, H. Shen, X. Fang, L. Fan, N. Zhao, J. Xu, Phase change materials of paraffin in h-BN porous scaffolds with enhanced thermal conductivity and form stability, Energy Build. 158 (2018) 1184–1188.
[38] X. Guo, S. Zhang, J. Cao, An energy-efficient composite by using expanded graphite stabilized paraffin as phase change material, Compos. A. Appl Sci. Manuf. 107 (2018) 83–93.
[39] Q. Huang, X. Li, G. Zhang, J. Deng, C. Wang, Thermal management of Lithium-ion battery pack through the application of flexible form-stable composite phase change materials, Appl. Therm. Eng. 183 (2021).
[40] N. Putra, S. Rawi, M. Amin, E. Kusrini, E.A. Kosasih, T.M. Indra Mahlia, Preparation of beeswax/multi-walled carbon nanotubes as novel shape-stable nanocomposite phase-change material for thermal energy storage, J. Energy Storage 21 (2019) 32–39.